Computational Study of Photonic Crystals Nano-Ring Resonator for Biochemical Sensing

Fu-li Hsiao and Chengkuo Lee, *Member, IEEE*

Abstract—We investigated the characteristics of photonic crystals (PCs) nano-ring resonators as biochemical sensors theoretically. The new nano-ring resonators were formed by removing holes of a hexagon from a two-dimensional (2-D) silicon PC slab in hexagonal lattice. Resonant peak with quality factor of about 3000 is reported. Biomolecules, e.g., DNAs, trapped in a hole functionalized with molecule probes made the wavelength shift of resonant peak derived in the output terminal. The sensitivity of various sensing holes along the nano-ring was characterized. This new PC nano-ring resonator demonstrated promising features as a biochemical sensor.

Index Terms—Biosensing, photonic crystal, ring resonator.

I. INTRODUCTION

OPTICAL sensing mechanisms receive considerable attention in the applications of chemical and biochemical sensors. Numerous optical chemical and biochemical sensors employed different sensing mechanisms such as directional couplers [1] and Bragg grating [2] have been reported. The sensing mechanisms are typically categorized into two main schemes. The first scheme is the detection of effective refractive index change in terms of homogeneous sensing, i.e., influenced by refractive index modification of covered medium. The second scheme is surface sensing, i.e., interfered by thickness change of thin biomolecular layer immobilized on surface [3], [4]. The label-free affinity-based optical biosensors allow us to study the selective binding between target molecules and captured agents without using a fluorescence or radio label. The commercially available label-free affinity-based optical biosensors detect selective binding by measuring the change in refractive index at the surface of the sensor with approaches such as surface plasmon resonance and colorimetric resonance in a diffractive grating surface. These approaches involve large area optical beams and a sensing area as large as 1 mm^2.

Micro-ring resonators which consist a ring waveguide sandwiched by two straight waveguides, i.e., bus and drop waveguides, have been reported as biosensors and biochemical sensors with good sensitivity due to high quality factor of resonant peak in output spectra [5]–[7]. De Vos *et al.* have reported detection of protein concentration down to 10 ng/ml based on a micro-ring resonator of 10×10 μm^2 size, while the concept of packaging this micro-ring resonator inside a microfluidic channel has been revealed as well [8]. The circular resonant mode of ring waveguide is excited by incoming light from bus waveguide, and the light of resonant wavelength will be coupled into drop waveguide eventually. Thus, output spectrum of drop port reveals a resonant peak. The refractive index change of ambient fluidics or biomolecules bound on the surface of ring waveguide leads to the variation of resonant condition hence it shifts the resonant wavelength. In order to enlarge the free space range and enhance the quality factor of micro-ring resonator, the reduction of ring radius is required. However, it results in obvious increment of bending loss of conventional dielectric micro-ring waveguide.

Photonic crystals (PCs) is an even more attractive sensing platform, because two-dimensional (2-D) silicon based PCs comprise a group of holes in a silicon slab to form a periodic dielectric structure which is compliant with photonic band gap (PBG). The propagation of light within PBG frequency range is forbidden in PCs structure [9], [10]. The light within the PBG frequency range is enabled to be guided or localized by introducing certain defects in the PCs structure. Therefore the local electromagnetic field is modified by surface state of holes, e.g., the various concentration of solution on top of PCs sensors. S. C. Buswell *et al.* demonstrated specific detection of proteins by sensing the cut-off wavelength of waveguide transmission mode based on 2-D PCs waveguides. Using immobilized biotin as probe, 2.5-nm-thick streptavidin film captured by biotin on the whole PC waveguide surface results in a 0.86 nm cutoff red-shift [11]. In contrast to the cutoff wavelength detection, measurement of resonant wavelength shift is a preferred sensing approach because the resonant peak of high quality factor enables high detection resolution.

With the aid of defects, microcavity or nanocavity based PCs resonators are demonstrated as PC sensors of high sensitivity in terms of resonant wavelength detection. First of all, PC resonator sensors are integrated in microbeams and microcantilevers for force and mechanical strain detection [12]–[14]. Secondly the resonant wavelength of PCs resonator sensors are extremely sensitive to a small refractive index change attributed to medium around hole surface. By using a 2-D PC microcavity based resonator, E. Chow *et al.* have demonstrated the measurement of ambient induced refractive index change via sensing

the resonant wavelength shift [15]. It has been reported that the similar 2-D PC microcavity resonator can detect protein down to 2.5 fg [16], a gold nanoparticle of 10 nm in diameter [17], and ion concentration absorbed in ion-selective polymer coated on the resonator [18]. Recently S. Zlatanovic reported detection limit of anti-biotin as less as 20 pM, corresponding to less than 4.5 fg of bound material on the sensor surface of 50 μm^2 and fewer than 80 molecules in the modal volume of the microcavity [19].

A Si waveguide nanocavity resonator comprising one-dimensional (1-D) periodic holes and a local defect, i.e., a missing hole, leads to a highly confined optical state. It has been reported that the Q factor of the resonant wavelength peak is measured as 265 [20]. This kind of Si waveguide nanocavity resonator has been investigated in terms of biosensors [21], [22]. The advantage of Si waveguide nanocavity resonator over the 2-D PC microcavity resonator is its much smaller sensor area. This view point leads to a concept that a nanocavity resonator with localized high electromagnetic field in PC will render resonant peak of high quality factor and access of efficient light-matter interaction regarding extremely small volumes of analyte, i.e., about 1 fL. On the other hand, the direct-write dip-pen nanolithography (DPN) can perform immobilization of protein and DNA in a nanometer scale patterns and holes [23], [24]. Such DPN technology gives us an opportunity of applying a single hole of micro/nanocavity of the PC resonators as the sensing element. As a result, specific biomolecule detection of captured a few molecules within a small hole of very small volume, e.g., 1 fL, can be technically realized. Recently, Intonti *et al.* reported a spectral tuning mechanism of photonic crystal microcavities based resonator by adding water into one or few holes in the microcavity area such that tunable resonator of high quality factor was demonstrated [25]. These evidences show that localized modification of surface state of one or more holes in a specific location in 2-D PCs is technically feasible.

In this paper, we propose a novel PCs based nano-ring resonator of hexagonal lattice for biomolecular sensing application and explore sensitivity upon a scenario of a single hole binding mechanism. Owning to the well light confinement, the size of hexagonal nano-ring resonator is as small as 3 μm^2. Comparing with the reported studies of PCs based microcavity sensors, we focus on the sensing phenomena in a single hole and the location of such a hole in between waveguide and nano-ring resonator.

II. RESONATOR CONFIGURATION AND OPTIMIZATION

In contrast to micro-ring resonator, 2-D PCs based nano-ring resonators provide very well optical confinement due to ultra low bending loss. Among the reported 2-D PCs based nano-ring resonators, devices of the cascaded cavities of point defect [26] and square ring defect [27], [28] have been studied. In comparison with the nano-ring resonators of square lattice, the bending angle of hexagonal nano-ring resonator is not as sharp as the square ring. The effect of counter-propagating mode [29] is significantly suppressed. Suspended InGaAsP membrane based microcavity of hexagonal lattice has been demonstrated as a refractive index sensor with quality factor as high as 6400 [30], while 2-D PCs resonator made of silicon based nano-rods of hexagonal lattice has been reported as a channel drop filter [31].
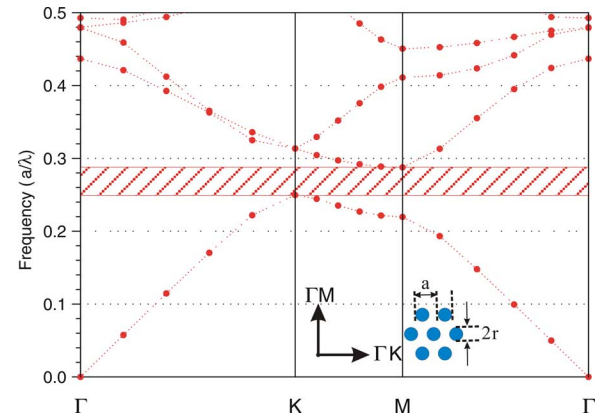

Fig. 1. Band structure of the PCs structure of hexagonal lattice (layout is shown as the inset); and the corresponding highest symmetric directions, i.e., ΓM and ΓK.

Hsiao and Lee have reported modeling results of silicon nano-ring resonator formed by having air holes in hexagonal lattice [32]. Characteristics of channel drop filter have been computationally explored. Briefly speaking, the 2-D PCs based hexagonal nano-ring resonators have higher filling factor than counterparts of square lattice, thus better intrinsic light confinement and wider band gap range can be obtained.

The 2-D PCs structure of hexagonal lattice is derived from the 220 nm thick device layer of a silicon-on-insulator (SOI) wafer. All surface of PCs structure is covered by water because the device is embedded in a microfluidic channel for biochemical sensing applications. The effective refractive index (ERI) approach and 2-D plane wave expansion (PWE) methods are employed to estimate the band gap of PCs structure as shown in Fig. 1. The inset of Fig. 1 denotes the lattice constant (a) of 410 nm and the radius of holes (r) of 120 nm. The ERI of silicon and water are 2.825 and 1.33, respectively. The two highest symmetric directions are denoted as ΓM and ΓK in Fig. 1. The band structure shows that the reduced first photonic band gap extends from 0.25 to 0.288 for TE polarized light, i.e., electric field is parallel to surface of silicon device layer. The corresponding wavelength range of the band gap is between 1423 and 1640 nm.

The coupled elements of PCs based waveguides and resonators have been applied to Fabry-Perot resonators formed by a short line defect in PCs structure [33]. The hybrid micro-ring resonator and PCs has been also reported [34]. In our design, the PCs based nano-ring resonator is formed by integrating terminal waveguides, i.e., line defects, and a hexagonal ring waveguide, i.e., a hexagon trace defect, as shown in Fig. 2(a). The bottom terminal waveguide is refereed as the bus waveguide which allows the input light from the left side of waveguide (marked by yellow arrow) to excite the resonant mode of the nano-ring resonator. Then the resonant light coupled to the upper terminal waveguide, i.e., the drop waveguide. ERI approach and 2-D finite-difference time-domain (FDTD) methods are employed to investigate the performance of nano-ring resonator. A temporal light pulse is launched into the bus waveguide. The output signal is recorded by a time monitor at the drop port or output port. The output spectrum is obtained by applying the Fast-Fourier Transform to the temporal signal recorded by the time monitor. Fig. 2(b) shows the output spectra of a nano-ring
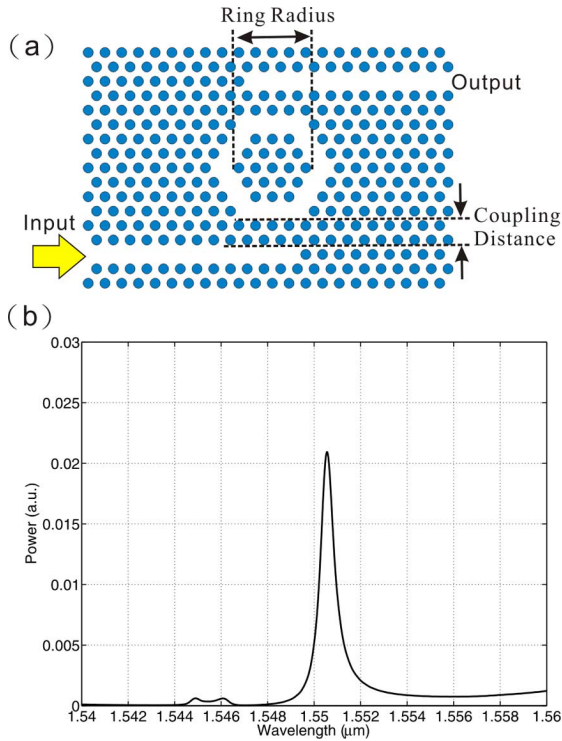
Fig. 2. (a) Layout sketch of the PCs based nano-ring resonator. (b) Output spectra of the PCs based nano-ring resonator in (a).
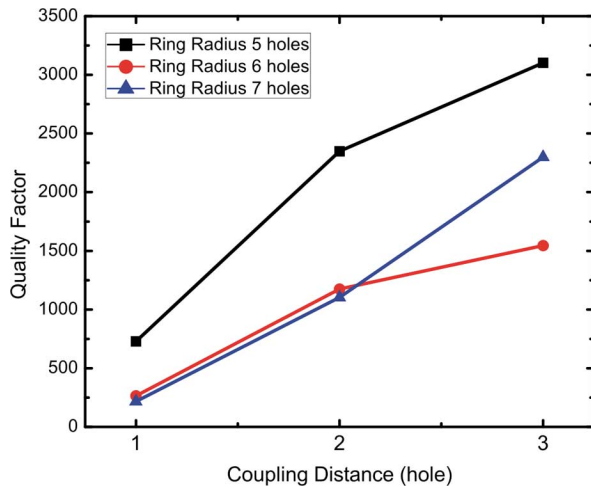

Fig. 3. Quality factors of the resonant peak varying with coupling distance. Black, red and blue line represents the quality factors of resonators with ring radii of five, six, and seven-hole, respectively.
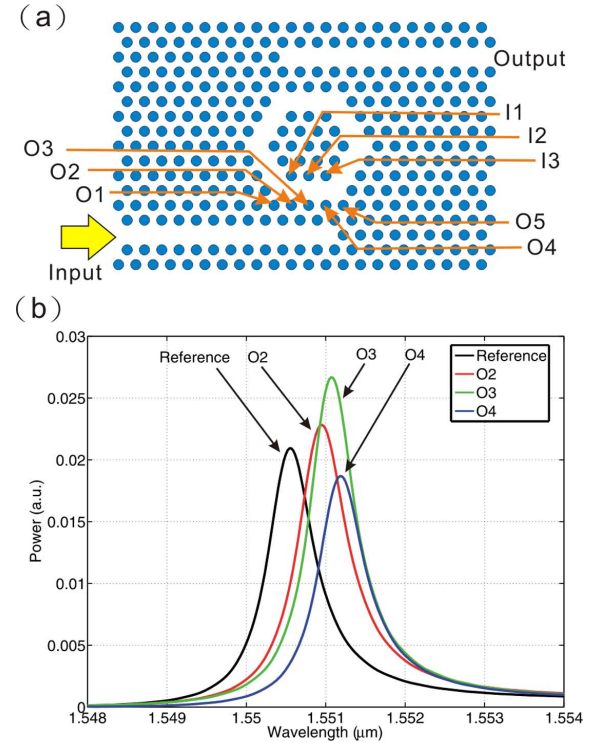

Fig. 4. (a) Layout sketch of a PCs based nano-ring resonator. Different positions of sensing hole are denoted by I1 to I3 and O1 to O5. (b) Output spectra of reference case and cases of biomolecules captured in O2, O3 and O4.

resonator as shown in Fig. 2(a). The resonant peak reveals at 1550.5 nm with the quality factor of around 2400.

The optimization of the performance of nano-ring resonator is performing by varying two geometric parameters, i.e., the ring radius and coupling distance [Fig. 2(a)]. For example, the ring radius is five-hole and the coupling distance is two-hole as shown in Fig. 2(a). Resonant wavelength and output spectra are changed with the variation of ring radius and coupling distance. According to various combinations of ring radii and coupling distances within the photonic band gap range, we choose the strongest spectral resonant peak as the major resonance. Fig. 3 demonstrates the quality factor of the major resonant peak of

nano-ring resonators with different coupling distance for three kinds of ring radii. The quality factors of ring radius of five, six, and seven-hole resonators are marked by black, red and blue lines, respectively. It shows that the quality factors are increased as the coupling distance arising. Larger coupling distance results in the improvement of light confinement hence it enhances the quality factor. Additionally the quality factors of the resonator with ring radius of five-hole are better than the other two cases for different coupling distances. The quality factor of resonators of five-hole ring radius and of two and three-hole coupling distance is derived as 2400 and 3200, respectively. Thus, we deployed these two resonator structures in our study in terms of biochemical sensing feasibility.

III. EVALUATION OF SENSING CHARACTERISTICS

A. Nano-Ring Resonator With Two-Hole Coupling Distance

Fig. 4(a) sketches the nano-ring resonator of two-hole coupling distance and five-hole ring radius. The nano-ring resonator is assumed to be packaged inside a fluidic channel. Particular holes at the boundary of resonator near the bus waveguide are investigated in terms of the ERI change inside a hole. Initially we consider all surface of resonator is covered by water, and the derived resonance peak is shown as the black peak in Fig. 4(b). Secondly a particular sensing hole is fully occupied with biomolecules, such as proteins and DNAs, i.e., the trapped analytes due to the biomolecule binding mechanism. The ERI in such a sensing hole is considered as 1.45. The positions of these sensing holes are marked in Fig. 4(a) as I1 to I3, and O1 to O5, because the holes of I1 to I3 and O1 to O5 means the holes located at the inner boundary and the outer

TABLE I
WAVELENGTH SHIFT AND QUALITY FACTOR

Sensing Holes	Wavelength shift (nm)	Quality factor
I1	0.05	2585
I2	0.05	2500
I3	0.1	2350
O1	0	2420
O2	0.4	2315
O3	0.55	2460
O4	0.65	2425
O5	0.05	2500

Note: List of wavelength shift and quality factor for different sensing holes of the nano-ring resonator as shown in Fig. 4(a).
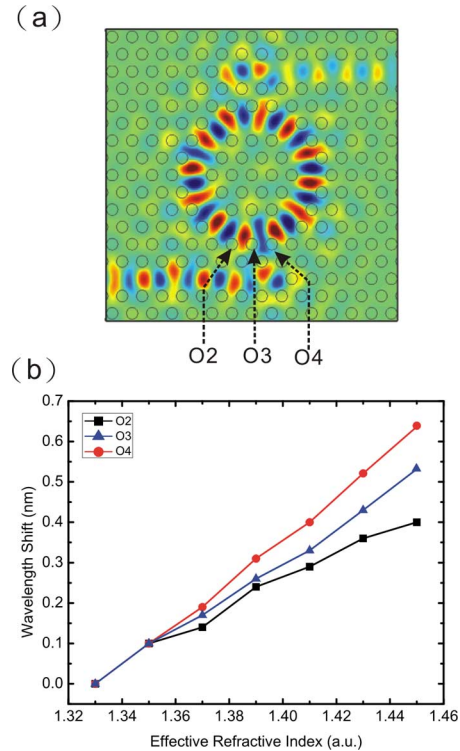

Fig. 5. (a) Out-of-plane magnetic field distribution of steady resonant modes. (b) Resonant wavelength varying with ERI of in different sensing holes O2 (black line), O3 (blue line), and O4 (red line). Computed model is predicted in Fig. 4(a).

boundary regarding to the nano-ring resonator, respectively. The scenario of detection of biomolecules of very small amount in a fluidic channel is that the biomolecules are carried by flow and transited trough the sensing hole. Selective binding mechanisms provided by antigen to antibody and DNA probe to DNA are deployed to capture these biomolecules in flow and to trap such biomolecules inside the sensing hole. When we investigated each individual hole as the sensing hole, the derived spectra are represented as red, green and blue peaks for cases of O2, O3, and O4, respectively. The resonant wavelength of these cases shifts to longer wavelength region, i.e., the red-shifted behavior, when each case has one sensing hole fully occupied with biomolecules. Both the resonant wavelength and peak intensity are related to the positions of sensing holes.

In fact, we have conducted the extensively investigation on position effect of sensing hole. The resonant wavelength shift and quality factor of resonant peak for resonators of individual sensing hole of I1 to I3 and O1 to O5 are shown in Table I. The results show that the wavelength shift is strongly dependent on the position of sensing holes. The most sensitive holes are O2, O3, and O4, while the largest wavelength shift is derived as 0.65 nm in the O4 case. In contrast, the biomolecule bound in the holes along the inner boundary of resonator only leads to slight resonant wavelength shift. The phenomenon implies that the resonance or light confinement condition of nano-ring resonator is mostly dominated by the outer boundary of ring. The strong dependence of position of sensing holes allows the feasibility in not only quantitative sensing but also the binding location detection. It is worth to notice that the quality factors do not fluctuate significantly in terms of the variation of position of sensing holes. It points out an advantage of maintaining the sensitivity and providing distinguished resolution during detection process.

To characterize the dependency of sensing hole location and resonator intrinsic behavior for cases of O2, O3 and O4, we calculated the steady resonant mode of this nano-ring resonator. The temporal light source in computed model of the spectra simulation is altered by a mono-frequency continue light source. The wavelength is set to be same with the resonant wavelength, i.e., the reference peak in Fig. 4(b) as of 1550.5 nm. The steady out-of-plane magnetic field is represented by a color map in Fig. 5(a). The fields in red and blue color are out of phase. The darkness of red or blue zone means the relevant intensity of localized light energy, i.e., the darker color is the stronger

intensity. The position of O2, O3, and O4 is denoted by the arrow marks. It shows that the strong magnetic field penetrated through the silicon matrix among O2, O3, and O4. Thus the resonance condition is sensitive to the alteration of ERI of these holes. On the other hand, there are not much energy distribute near the holes at O1, O5, I1, I2, and I3, such that the ERI variation inside these holes does not give rise to significant effect upon the resonance condition.

Furthermore, the relation between resonant wavelength shifting and the variation of ERI (from 1.33 to 1.45) of sensing holes is investigated for the three most sensitive holes, i.e., O2, O3, and O4. The results are shown at Fig. 5(b). The black, blue and red lines indicate the trend of wavelength shift as a linear function of the ERI change in hole O2, O3 and O4, respectively. With an assumption that the trapped biomolecules are in homogenous distribution within a sensing hole of 240 nm in diameter, the wavelength shift is in proportion to the ERI derived in the sensing hole. The smaller ERI within the sensing hole refers to the case that the density of DNA inside the sensing hole becomes smaller. The ERI of 1.45 in the sensing hole means that the hole is fully filled by biomolecules. Referring to the average density of DNA molecules as of 0.15 pg/m^3 [35], the derived weight of DNA molecules inside a sensing hole is about 1.5 fg. In the case of homogenous distribution of DNA molecules in the sensing hole, the ERI of 1.35 in a sensing hole refers to the case that there are DNA molecules of 0.25 fg inside a sensing hole. We can define the sensitivity as resonant wavelength shift, i.e., nm, per biomolecule weight in unit of fg. As a result, the sensitivity of nano-ring resonator with a sensing
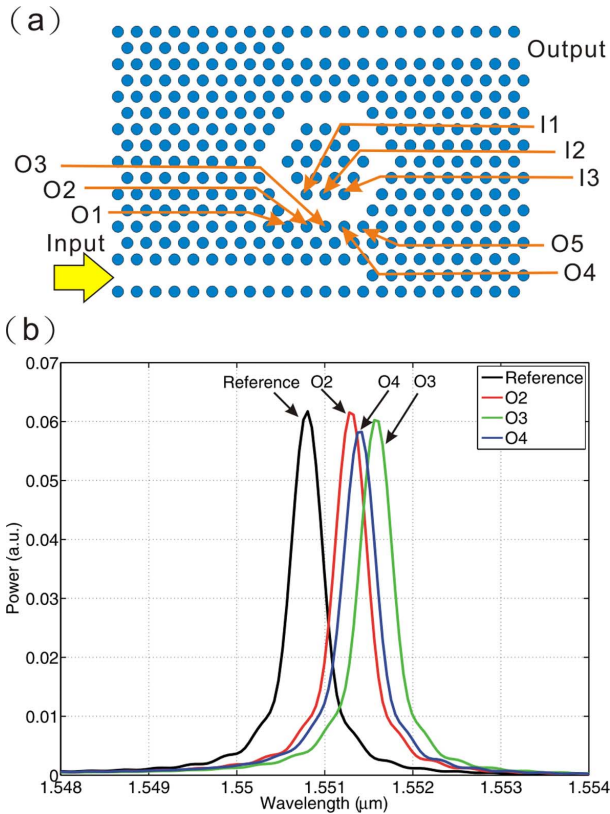
（a）

（b）

Fig. 6. (a) Layout sketch of a PCs based nano-ring resonator with five-hole ring radius and three-hole coupling distance. Different positions of sensing hole are denoted as I1 to I3 and O1 to O5. (b) Spectra of reference peak and peaks of the cases that biomolecules trapped in a sensing hole of O2, O3, and O4.

TABLE II
WAVELENGTH SHIFT AND QUALITY FACTOR

Sensing Holes	Wavelength shift (nm)	Quality factor
I1	0.05	3200
I2	0.05	3290
I3	0.05	3120
O1	0	3200
O2	0.45	3200
O3	0.75	3200
O4	0.58	3040
O5	0.05	3200

List of wavelength shift and quality factor for different sensing holes of the nano-ring resonator as shown in Fig. 6(a).
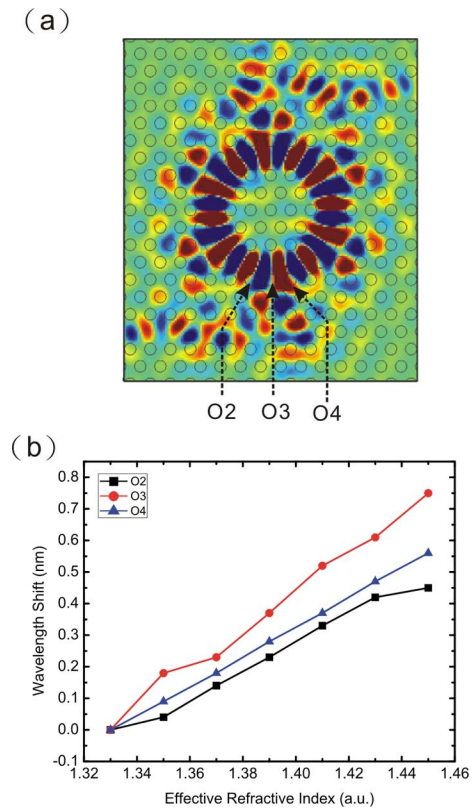
（a）

（b）

Fig. 7. (a) Out-of-plane magnetic field distribution of steady resonant modes. (b) Resonant wavelength varying with ERI of sensing holes O2 (black line), O3 (red line) and O4 (blue line). Computed model is predicted in Fig. 6(a).

hole at O2, O3, and O4 is derived as 0.26, 0.36, and 0.43 nm/fg, respectively. With respect to 0.1 nm resolution provided by most commercial measurement tools, the minimum detectable biomolecule weight in the sensing hole O4 for a nano-ring resonator of five-hole ring radius and two-hole coupling distance is derived as 0.23 fg.

B. Nano-Ring Resonator With Three-Hole Coupling Distance

We further studied another nano-ring resonator structure with larger coupling distance, i.e., 3 holes. Fig. 6(a) shows this resonator with sensing holes of I1 to I3 and O1 to O5 as same as the locations defined in Fig. 4(a). The simulation process follows the same procedure as we conducted for nano-ring resonator with two-hole coupling distance. As shown in Fig. 6(b), the reference black peak at 1550.8 nm and with the quality factor of around 3200 is the resonant peak obtained when nano-ring resonator is covered by pure water. The red, green and blue peaks are the output spectra derived for nano-ring resonator of three-hole coupling distance for the sensing hole at O2, O3, and O4, respectively. Again, we considered the sensing hole is filled by biomolecules, while the ERI in such a sensing hole is considered as 1.45. Table II lists the wavelength shift and quality factor derived for nano-ring resonator using individual sensing hole as depicted in Fig. 6(a). The results of Fig. 6(b) and Table II show that the most sensitive resonator configurations are still referring to sensing holes of O2, O3, and O4, in which it is the same as the observation in Fig. 4(b) and Table I. However, the most

sensitive hole is O3 in Table II but not the O4 in Table I, while the quality factor maintain above 3000 in all cases in Table II. In comparison of Figs. 6(b) and 4(b), the intensity difference among different resonant peaks in Fig. 6(b) is smaller than the difference observed in Fig. 4(b). It facilitates the measurement of fabricated nano-ring resonator in future. Besides, the output intensity of resonant peaks in Fig. 6(b) is about two times higher than the ones in Fig. 4(b). It indicates that the nano-ring resonator of three-hole coupling distance as shown in Fig. 6(a) reveals better drop efficiency.

Fig. 7(a) shows the out-of-plane magnetic field of the steady resonant mode of the nano-ring resonator of three-hole coupling distance as shown in Fig. 6(a). The magnetic field distribution reveals that the light energy penetrates deeply into the holes O2,

O3, and O4. Especially, most of light coupled from bus waveguide into ring resonator is through the surrounding area of the sensing hole O3. It provides a rational explanation about why the highest wavelength shift is observed for the sensing hole O3. Fig. 7(b) shows the trend of wavelength shift as a function of the ERI change in holes O2, O3, and O4. All cases show data in linear proportion to the ERI change. As mentioned before, the sensitivity of nano-ring resonators of three-hole coupling distance with various sensing holes at O2, O3, and O4 is derived as 0.3, 0.5, and 0.38 nm/fg, respectively. The minimum detectable biomolecule weight in the sensing hole O3 for a nano-ring resonator of five-hole ring radius and three-hole coupling distance is derived as 0.2 fg. It means 15% improvement is observed for a nano-ring resonator of three-hole coupling distance than the one of two-hole coupling distance in terms of the minimum detectable biomolecule weight. According to this calculated detection limit, it is about ten times better than previous reported data [16], [19]. In future implementation, a lab-on-a-chip (LoC) device comprising microfluidic channel integrated on the nano-ring resonator is expected as a promising sensor for biochemical sensing such as DNA and protein detection. LoC device with detection resolution down to 0.2 fg will play important role in point-of-care diagnostics and rapid drug screening applications.

IV. CONCLUSION

In summary, we demonstrated the feasibility of a PCs-based nano-ring resonator for biochemical sensing applications. The nano-ring resonator comprises hexagonal waveguide and two terminal waveguides in a 2-D silicon PCs substrate of hexagonal lattice when we considered the whole resonator is embedded inside a microfluidic channel. The proposed nano-ring resonator combines advantages of ring resonator and 2-D PCs such that it reveals high quality factor, small footprint and very high sensitivity. The geometric configuration of nano-ring resonator was optimized. The results show that the higher coupling distance enhances the quality factor and drop efficiency. The quality factors of the nano-ring resonators of two-hole and three-hole coupling distances are derived as 2400 and 3200, respectively. We also investigated the sensitivity for the nano-ring resonators of two-hole and three-hole coupling distances in terms of the position sensing holes. The resonant wavelength shift shows strong dependence on the position of sensing holes and linear proportion to the ERI change within the sensing hole. The minimum detectable biomolecule weight in a sensing hole for a nano-ring resonator of two-hole and three-hole coupling distance is derived as 0.23 fg and 0.2 fg, respectively. It shows promising applications which demands detection of biomolecules down to the level of single copy of DNA.

REFERENCES

[1] B. J. Luff, R. D. Harris, J. S. Wilkinson, R. Wilson, and D. J. Schiffrin, "Integrated-optical directional coupler biosensor," *Opt. Lett.*, vol. 21, no. 8, pp. 618–620, 1996.

[2] W. C. L. Hopman, P. Pottier, D. Yudistira, J. van Lith, P. V. Lambeck, R. M. De La Rue, A. Driessen, H. J. W. M. Hoekstra, and R. M. de Ridder, "Quasi-one-dimensional photonic crystal as a compact building-block for refractometric optical sensors," *IEEE J. Sel. Top. Quantum Electron.*, vol. 11, no. 1, p. 11, 2005.

[3] F. Dell'Olio and V. M. N. Passaro, "Optical sensing by optimized silicon slot waveguides," *Opt. Expr.*, vol. 15, no. 8, pp. 4977–4993, 2007.

[4] N. Skivesen, A. Têtu, M. Kristensen, J. Kjems, L. H. Frandsen, and P. I. Borel, "Photonic-crystal waveguide biosensor," *Opt. Expr.*, vol. 15, no. 6, pp. 3169–3176, 2007.

[5] E. Krioukov, D. J. W. Klunder, A. Driessen, J. Greve, and C. Otto, "Sensor based on an integrated optical microcavity," *Opt. Lett.*, vol. 27, no. 7, pp. 512–514, 2002.

[6] C. Y. Chao, W. Fung, and L. J. Guo, "Polymer microring resonators for biochemical sensing applications," *IEEE J. Sel. Top. Quantum Electron.*, vol. 12, no. 1, pp. 134–142, 2006.

[7] M. Kwon and W. H. Steier, "Microring-resonator-based sensor measuring both the concentration and temperature of a solution," *Opt. Expr.*, vol. 16, no. 13, pp. 9372–9377, 2008.

[8] K. De Vos, I. Bartolozzi, E. Schacht, P. Bienstman, and R. Baets, "Silicon-on-Insulator microring resonator forsensitive and label-free biosensing," *Opt. Expr.*, vol. 15, no. 12, pp. 7610–7615, 2007.

[9] E. Yablonovitch, "Inhibited spontaneous emission in solid-state physics electronics," *Phys. Rev. Lett.*, vol. 58, no. 20, pp. 2059–2062, 1987.

[10] S. John, "Strong localization of phonics in certain disordered dielectric Superlattices," *Phys. Rev. Lett.*, vol. 58, no. 23, pp. 2486–2489, 1987.

[11] S. C. Buswell, V. A. Wright, J. M. Buriak, V. Van, and S. Evoy, "Specific detection of proteins using photonic crystal waveguides," *Opt. Expr.*, vol. 16, no. 20, pp. 15949–15957, 2008.

[12] C. Lee, R. Radhakrishnan, C. C. Chen, J. Lin, J. Thillaigovindan, and N. Balasubramanian, "Design and modeling of a nanomechanical sensor using silicon photonic crystals," *J. Lightw. Technol.*, vol. 26, pp. 839–846, Apr. 2008.

[13] C. Lee, J. Thillaigovindan, C.-C. Chen, X. T. Chen, Y.-T. Chao, S. Tao, W. Xiang, A. Yu, H. Feng, and G. Q. Lo, "Si nanophotonics based cantilever sensor," *Appl. Phys. Lett.*, vol. 93, p. 113113, 2008.

[14] C. Lee and J. Thillaigovindan, "Optical nanomechanical sensor using Si photonic crystals cantilever embedded with nanocavity resonator," *Appl. Opt.*, vol. 48, pp. 1797–1803, Apr. 2009.

[15] E. Chow, A. Grot, L. W. Mirkarimi, M. Sigalas, and G. Girolami, "Ultracompact biochemical sensor built with two-dimensional photonic crystal microcavity," *Opt. Lett.*, vol. 29, no. 10, pp. 1093–1095, 2004.

[16] M. Lee and P. M. Fauchet, "Two-dimensional silicon photonic crystal based biosensing platform for protein detection," *Opt. Expr.*, vol. 15, no. 8, pp. 4530–4535, 2007.

[17] M. R. Lee and P. M. Fauchet, "Nanoscale microcavity sensor for single particle detection," *Opt. Lett.*, vol. 32, no. 22, pp. 3284–3286, 2007.

[18] S. Chakravarty, J. Topol'ancik, P. Bhattacharya, S. Chakrabarti, Y. Kang, and M. E. Meyerhoff, "Ion detection with photonic crystal microcavities," *Opt. Lett.*, vol. 30, no. 9, pp. 2578–2580, 2005.

[19] S. Zlatanovic, L. W. Mirkarimi, M. M. Sigalas, M. A. Bynum, E. Chow, K. M. Robotti, G. W. Burr, S. Esener, and A. Grot, "Photonic crystal microcavity sensor for ultracompact monitoring of reaction kinetics and protein concentration," *Sens. Actuators B*, vol. 141, pp. 13–19, 2009.

[20] J. S. Foresi, P. R. Villeneuve, J. Ferrera, E. R. Thoen, G. Steinmeyer, S. Fan, J. D. Joannopoulos, L. C. Kimerling, H. I. Smith, and E. P. Ippen, "Photonic-bandgap microcavities in optical waveguides," *Nature*, vol. 390, pp. 143–145, 1997.

[21] C. Lee, A. S. P. Yee, J. L. J. Perera, C.-C. Chen, and N. Balasubramanian, "Design of nanobiophotonics resonators for biomolecules detection," in *Proc. 3rd Annu. IEEE Int. Conf. Nano/Micro Engineered and Molecular Systems*, Sanya, China, Jan. 6–9, 2008, pp. 274–279.

[22] S. Mandal and D. Erickson, "Nanoscale optofluidic sensor arrays," *Opt. Expr.*, vol. 16, no. 3, pp. 1623–1631, 2008.

[23] S.-W. Chung, D. S. Ginger, M. W. Morales, Z. Zhang, V. Chandrasekhar, M. A. Ratner, and C. A. Mirkin, "Top-down meets bottom-up: Dip-pen nanolithography and DNA-directed assembly of nanoscale electrical circuits," *Small*, vol. 1, no. 1, pp. 64–69, 2005.

[24] J. Haaheim, R. Eby, M. Nelson, J. Fragala, B. Rosner, H. Zhang, and G. Athas, "Dip pen nanolithography (DPN): Process and instrument performance with NanoInk's NSCRIPTOR system," *Ultramicrosc.*, vol. 103, no. 2, pp. 117–132, 2005.

[25] F. Intonti, S. Vignolini, F. Riboli, M. Zani, D. S. Wiersma, L. Balet, L. H. Li, M. Francardi, A. Gerardino, A. Fiore, and M. Gurioli, "Tuning of photonic crystal cavities by controlled removal of locally infiltrated water," *Appl. Phys. Lett.*, vol. 95, p. 173112, 2009.

[26] S. Fan, P. R. Villeneuve, J. D. Joannopoulos, and H. A. Haus, "Channel drop filters in photonic crystals," *Opt. Expr.*, vol. 3, pp. 4–11, 1998.

[27] Z. Qiang, W. Zhou, and R. A. Soref, "Optical add-drop filters based on photonic crystal ring resonators," *Opt. Expr.*, vol. 15, pp. 1823–1831, 2007.

[28] F. Monifi, A. Ghaffari, M. Djavid, and M. S. Abrishamian, "Three output port channel-drop filter based on photonic crystals," *Appl. Opt.*, vol. 48, pp. 804–809, 2009.

[29] V. Kumar, T. Srinivas, and A. Selvarajan, "Investigation of ring resonators in photonic crystal circuits," *Photon. Nanostruct.*, vol. 2, pp. 199–206, 2004.

[30] T.-W. Lu, Y.-H. Hsiao, W.-D. Ho, and P.-T. Lee, "Photonic crystal hetero-slab-edge microcavity with high quality factor surface mode for index sensing," *Appl. Phys. Lett.*, vol. 94, p. 141110, 2009.

[31] W. Y. Chiu, T. W. Huang, Y. H. Wu, Y. J. Chan, C. H. Hou, H. T. Chien, and C. C. Chen, "A photonic crystal ring resonator formed by SOI nano-rods," *Opt. Expr.*, vol. 15, pp. 15500–15506, 2007.

[32] F.-L. Hsiao and C. Lee, "A nano-ring resonator based on 2-D hexagonal-lattice photonic crystals," in *Proc. IEEE/LEOS Int. Conf. on Optical MEMS and Nanophotonics*, Clearwater Beach, FL, Aug. 17–20, 2009, pp. 107–108.

[33] M. Notomi, A. Shinya, S. Mitsugi, E. Kuramochi, and H. Y. Ryu, "Waveguides, resonators and their coupled elements in photonic crystal slabs," *Opt. Expr.*, vol. 12, no. 8, pp. 1551–1561, 2004.

[34] D. Goldring, U. Levy, and D. Mendlovic, "Highly dispersive micro-ring resonator based on one dimensional photonic crystal waveguide design an analysis," *Opt. Expr.*, vol. 15, no. 6, pp. 3156–3168, 2007.

[35] M. D. Bennett, J. S. Heslop-Harrison, J. B. Smith, and J. P. Ward, *DNA Density in Mitotic and Meiotic Metaphase Chromosomes of Plants and Animals*, vol. 63, no. 1, pp. 173–179, 1983.

Fu-Li Hsiao received the B.S. degree from the Department of Physics, National Changhua University of Education, Changhua City, Taiwan, in 2002 and the Ph.D. degree from FEMTO-ST, University of Franche-Comte, France, and from the Department of Optics and Photonics, National Central University, Taiwan, in 2008.

He was a Research Fellow with the Department of Electrical and Computer Engineering, National University of Singapore, from November 2008 to July 2009. Currently, he is an Assistant Professor with the Graduate Institute of Photonics, National Changhua University of Education. His research interests include photonic crystals, phononic crystals, and optical MEMS.

Chengkuo Lee (M'96) received the M.S. degree in materials science and engineering from National Tsing Hua University, Hsinchu, Taiwan, in 1991, the M.S. degree in industrial and system engineering from Rutgers University, New Brunswick, NJ, in 1993, and the Ph.D. degree in precision engineering from the University of Tokyo, Tokyo, Japan, in January 1996.

He was a Foreign Researcher in the Research Center for Advanced Science and Technology (RCAST), University of Tokyo, in 1996. He was also with the Mechanical Engineering Laboratory, AIST, MITI of Japan, as a Research Fellow in 1996. Thereafter, he was a Senior Research Staff at the Microsystems Laboratory, Industrial Technology Research Institute, Hsinchu, Taiwan. Since September 1997, he has been with the Metrodyne Microsystem Corporation, Hsinchu, Taiwan, and he established the MEMS Device Division and micromachining fabrication. He was the Manager of MEMS Device Division from 1997 to 2000. He was an Adjunct Assistant Professor in the Electro-Physics Department, National Chiao Tung University, in 1998, and an Adjunct Assistant Professor in the Institute of Precision Engineering, National Chung Hsing University, from 2001 to 2005. He cofounded Asia Pacific Microsystems, Inc., (APM) Hsinchu, Taiwan, in August 2001, and he became the Vice President (VP) of R&D, then the VP of the Optical Communication Business Unit. Currently, he is an Assistant Professor at the Department of Electrical and Computer Engineering, National University of Singapore, and a Senior Member of Technical Staff at the Institute of Microelectronics (IME), Agency for Science, Technology, and Research (A*STAR), Singapore. He has contributed more than 200 international conference papers and international journal articles in the MEMS and nanotechnology fields.

Dr. Lee is a member of MRS and IEE Japan. He received the IUMRS Graduate Student Award in 1994.